

D.C conductivity of In₂O₃: SnO₂ thin films and manufacturing of gas sensor

Bushra A. Hasan and Rusul M. Abdallah

Department of Physics, College of Science, University of Baghdad

E-mail: bushra_abhasan@yahoo.com

Abstract

Compounds were prepared from In₂O₃ doped SnO₂ with different doping ratio by mixing and sintering at 1000°C. Pulsed Laser Deposition PLD was used to deposit thin films of different doping ratio In₂O₃: SnO₂ (0, 1, 3, 5, 7 and 9 % wt.) on glass and p-type wafer Si(111) substrates at ambient temperature under vacuum of 10⁻³ bar thickness of ~100nm. X-ray diffraction and atomic force microscopy were used to examine the structural type, grain size and morphology of the prepared thin films. The results show the structures of thin films was also polycrystalline, and the predominate peaks are identical with standard cards ITO. On the other side the prepared thin films declared a reduction of degree of crystallinity with the increase of doping ratio. Atomic Force Microscopy (AFM) measurements show the average grain size exhibit to change in non-systematic manner with the increase of doping ratio with tin oxide. The average grain size increases at doping ratios 1, 5 and 7 % from 52.48 to 79.12, 87.57, and 105.59 nm respectively and decreases at residual doping ratio. The average surface roughness increases from 0.458 to 26.8 nm with the increase of doping ratio. The gas sensing measurements of In₂O₃:SnO₂ thin films prepared on p-Si to NO₂ gas showed good sensitivity and Maximum sensitivity (50) obtained for In₂O₃:SnO₂ prepared on p-Si at operating temperature 573 K and doping ratio 7 % and 9 %. Maximum speed of response time (8 sec) at operating temperature 573 K and doping ratio 1 %.

Key words

Thin films of In₂O₃:SnO₂, XRD, AFM, PLD, thin films gas sensors.

Article info.

Received: Sep. 2017

Accepted: Nov. 2017

Published: Jun. 2018

التوصيلية الكهربائية المستمرة وتصنيع متحسس غازي من اغشية اوكسيد الانديوم المطعم

باوكسيد القصدير

بشرى عباس حسن و رسل محمد عبدالله

قسم الفيزياء، كلية العلوم، جامعة بغداد

الخلاصة

حضرت مركبات من اوكسيد الانديوم المطعم باوكسيد القصدير وبنسب تطعيم مختلفة وذلك بمزج المركبين وتليدها عند درجة 1000 °C. تم استخدام طريقة التبخير بالليزر النبضي لتحضير اغشية رقيقة من المركب In₂O₃:SnO₂ وبنسب تطعيم (0, 1, 3, 5, 7, 9 % wt.) على قواعد من الزجاج ورقائق السليكون مفرد البلورة. وعند درجة حرارة المحيط وعند ضغط فراغ 10⁻³ تور وبسلك 150 نانوميتر. تم استخدام حيود الاشعة السينية ومطياف القوى الذرية لفحص تركيب، الحجم الحبيبي وطبوغرافية الاغشية المحضرة. اظهرت النتائج ان الاغشية المحضرة كانت متعددة البلورة وان المستوي المفضل للنمو متطابق مع بطاقات اوكسيد الانديوم- القصدير ومن جهة اخرى اظهرت الاغشية المحضرة هبوطا في درجة التبلور مع زيادة نسبة التطعيم. قياسات مطياف القوى الذرية اظهرت ان حجم الحبيبة تغير بشكل غير منتظم مع نسبة التطعيم. حيث ازداد حجم

الحبيبة عند نسب التطعيم % 1, 5, 7 من 52 الى 79، 87 و 105 نانوميتر على التوالي وهبط عند نسب التطعيم الباقية. خشونة السطح ازدادت من 0.458 الى 26.8 نانوميتر مع زيادة نسبة التطعيم. قياسات التحسس لآغشية $\text{In}_2\text{O}_3:\text{SnO}_2$ المحضرة على قواعد من السليكون نوع p لغاز NO_2 كانت جيدة و اقصى قيمة للتحسس كانت (50) لآغشية $\text{In}_2\text{O}_3:\text{SnO}_2$ المحضرة عند درجة تشغيل 573 K ونسب تطعيم % 7، 9%. اقصى زمن استجابة كان (8 sec) عند درجة تشغيل 573 K ونسبة تطعيم 1%.

Introduction

One of the most important semiconductors is the so-called transparent conductive oxides (TCO), which are compound semiconductors composed of Oxygen combined with metal (i.e semiconductor oxides). Transparent Conducting Oxide (TCO) films have been used extensively in the optoelectronics industry because they exhibit high electrical conductivity, high optical transmittance in the visible region, and high reflectance in the infrared (IR) region [1]. Although most research on TCO materials has been focused on the above oxides, there have been some efforts on making multicomponent oxides to improve the electrical conductivity and optical transparency of the films, such as $\text{In}_2\text{O}_3\text{-ZnO}$, $\text{In}_2\text{O}_3\text{-SnO}_2$, $\text{Ga}_2\text{O}_3\text{-In}_2\text{O}_3$ [2]. $\text{In}_2\text{O}_3:\text{SnO}_2$ (ITO) thin films have been receiving significant attention in several applications due to their attractive properties such as high transmittance in visible region and unique electrical conductivity, which originates from its n-type highly degenerate semiconductor behavior with a wide band gap in the range between 3.5 and 4.3 eV [3, 4]. ITO has been widely applied in various optoelectronic devices such as photovoltaic cells [5], liquid crystal displays [6] and gas sensors [7]. $\text{In}_2\text{O}_3\text{-SnO}_2$ is the most used n-type semiconductor in gas sensing devices because of its capabilities to detect inflammable gases like CH_4 , H_2 , $\text{C}_2\text{H}_5\text{OH}$, CO and so on [8]. Besides, Indium Tin oxide ($\text{In}_2\text{O}_3:\text{SnO}_2$) nano composites that exhibited superior thermal stability against grain growth have been reported [9]. It is difficult

to control the size and morphology of the oxide composites, which have important influence on their physical and chemical properties. There are many deposition techniques to obtain high quality ITO films such as pulsed laser deposition [10], sol-gel [11], RF and DC sputtering [12, 13].

The current research devoted with preparation of ITO films by PLD on glass substrate and The morphology, structural and composition analysis of ITO films were examined and the sensing properties of un-doped In_2O_3 and doped with different concentrations (1, 3, 5, 7 and 9) % of SnO_2 films deposited on p-type silicon wafer(111) are examined as a function of operating temperature and time to find the temperature dependence of the sensitivity for oxidizing gas (NO_2).

Experimental part

$\text{In}_2\text{O}_3:\text{SnO}_2$ is were prepared by quenching technique. Takes appropriate amount the of high purity (99.99) Indium oxide powder and doping with different percentages of tin oxide 99.9 % (are weighed using an electronic balance with the least count of 10^{-4} gm) and put in a quartz ampoule (length ~ 25 cm and internal diameter ~ 8 mm) are heated to 1000 °C and let at this temperature for 8 hours. The temperature of the furnace was raised at a rate of 10 °C/min. During heating the ampoules are constantly agitated .This is done to obtain homogeneous compound. Si wafer cut in small pieces (1×1) cm^2 . Cleaning glass slides and Si wafer substrates were used which were subjected to several steps to remove

any contamination such as dust, oily material, grease and some oxides using soap solution, then the glass slides and Si were placed in a clean beaker containing distilled water and with ethanol solution then the glass slides and Si were dried by blowing air. Thin films were deposited using pulsed laser deposition technique under vacuum of (10^{-3} Torr). Thin films were obtained by focusing Nd:YAG type (Huafei Tongda Technology-Diamond- 288 pattern EPLS). The characteristics of the laser tool were (1) Laser model: Q-switched Nd: YAG Laser Second Harmonic Generation (SHG). Laser wavelength: (1064 /532) nm. (2)Pulse energy: (100-1000) mJ. (3)Pulse width: 10ns. (4) Repetition frequency: (1, 2, 3, 4, 5, 6) Hz. (5) Cooling method: inner circulation water cooling and (6) Applied voltage: 220 V. The laser beam which coming from a window is incident on the target surface making an angle of 45° with it. The substrate is placed in front of the target with its surface parallel to that of the target. The structure of the prepared alloys and thin films was examined using X-ray diffraction (XRD). The present work x-ray diffractometer type (Miniflex II), with Cu-K α x-ray tube ($\lambda = 1.54056 \text{ \AA}$) is used. The resistivity of pure In₂O₃ and In₂O₃:SnO₂ thin films with different composition ratios prepared on glass substrate estimated by DC measurements after depositing metal electrodes (Al) on the samples using appropriate masks. The method comprises a temperature controller oven. The films glass samples are heated in the oven from room temperature up to 473 K with step of 298K. Electrical resistance is then measured directly with digital electrometer. The resistivity is conventionally calculated from measured electrical resistance. The

activation energy is calculated using equations.

The resistivity (ρ) of the films is calculated using the following equation:

$$\rho = \frac{R.A}{L}$$

where R is the sample resistance, A is the cross section area of the films and L is the distance between the electrodes. The conductivity of the films was determined from the relation:

$$\sigma_{d.c} = \frac{1}{\rho} \quad (1)$$

The activation energies could be calculated from the plot of $\ln \sigma$ versus $1000/T$ according to equation

$$\sigma = \sigma_0 \exp\left(-\frac{E_a}{k_B T}\right) \quad (2)$$

where σ_0 is the minimum electrical conductivity at 0 °K, E_a is the activation energy which corresponds to ($E_g/2$) for intrinsic conduction, T is the absolute temperature and k_B is the Boltzman's constant equal ($8.617 \times 10^{-5} \text{ eVK}^{-1}$). By taking (Ln) of the two sides of equation we can get:

$$\ln \sigma = \ln \sigma_0 - (E_a / k_B T) \quad (3)$$

From determination of the slope we can find the activation energy

$$E_a = k_B \cdot \text{slope} \quad (4)$$

The conductivity type of the thin films is deduced using Hall measurement. Hall Effect measurements have been used in determining majority carrier concentrations, type of carrier and their mobility in thin film materials. The values of carrier concentration (n_H) and Hall mobility (μ_H) were calculated using equations:

$$n_H = \frac{-1}{R_H \cdot q} \quad (5)$$

$$\mu_H = \sigma |R_H| \quad (6)$$

$$\text{where } R_H = \frac{V_H}{I} * \frac{t}{B} \quad (7)$$

RH is Hall coefficient, VH is Hall

voltage, t is the sample of thickness, I is constant current, σ is conductivity, and B is magnetic field.

In this work, the gas responsivity tests performed at different operation temperature beginning from (room temperature, 373, 473 and 573) °C. The time taken for the sensor to attain 90 % of the maximum increase in resistance on exposure to the target gas is the response time. The time taken for the sensor to get back 90 % of original resistance is the recovery time. The test was performed at various sensing temperatures with 6 V bias voltage. The sensitivity factor (S %) at different operating temperatures is calculated using equation:

$$S = \left| \frac{R_a - R_g}{R_a} \right| = \frac{\Delta R}{R_a} \dots \quad (8)$$

for oxidizing gases.

Results and discussion

1-Structural properties

The diagram of the X-ray diffraction spectra of In_2O_3 thin films deposited on glass substrates prepared by the PLD technique with different doping concentrations of SnO_2 (1, 3, 5, 7 and 9) wt. % showed in Fig.1. All the peaks of XRD patterns were analyzed and indexed using JCPDS data base and compared with standards (JCPDS-#06-0416). XRD diffractograms revealed that $\text{In}_2\text{O}_3:\text{SnO}_2$ films become polycrystalline when deposited at room substrate temperature and crystallize in a cubic bixbyite structure (In_2O_3). The peaks observed for ($2\theta = 30.4^\circ$) associated to the plane (222) and other planes related to the ITO system likes (400) (440) and (622). The preferential growth of the $\text{In}_2\text{O}_3:\text{SnO}_2$ films is the (222) plane and this orientation should be dependent on the deposition conditions. The similar result was reported using an evaporation method [14].

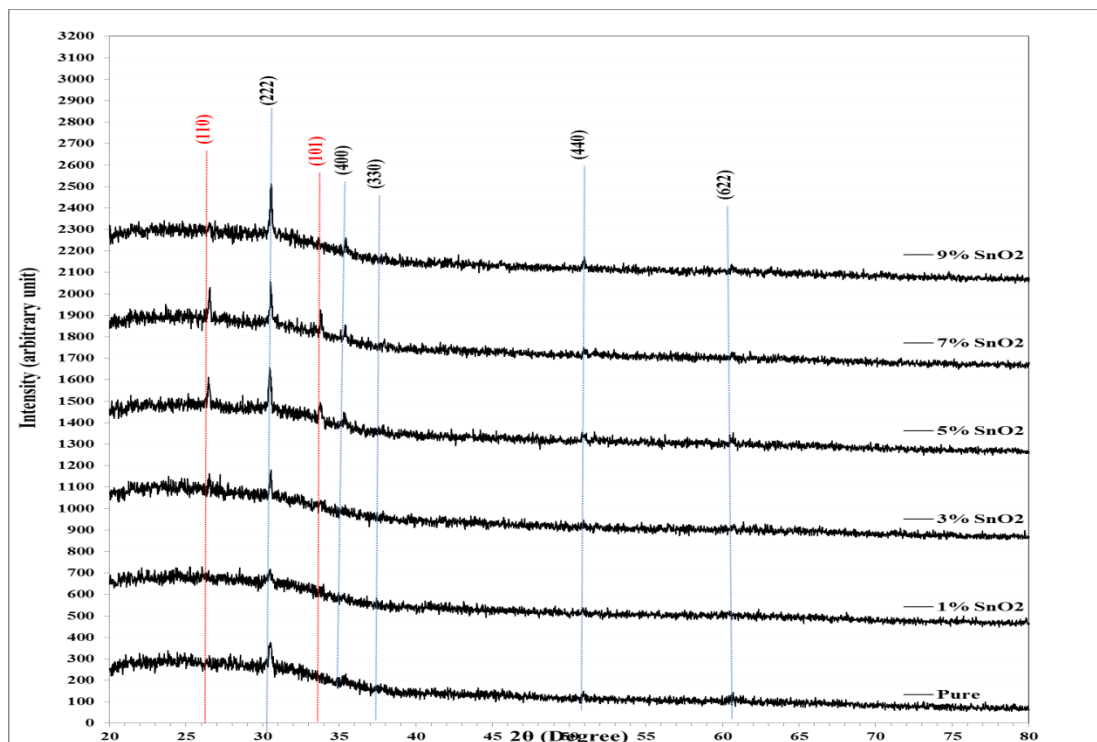


Fig.1: X-ray diffraction patterns of deposited In_2O_3 undoped and doped by SnO_2 at different ratio (1, 3, 5, 7 and 9) %.

2- Atomic Force Microscopy analysis (AFM)

Atomic Force Microscopy (AFM) was employed to study the surface morphologies of $In_2O_3:SnO_2$ films. Fig.2 shows their surface morphologies analyzed by AFM. The measured grain size and RMS roughness are illustrates an increment in average diameter with doping ratio 1% (at pure =52.48 and at

1% =100.22) then go down in 3% (79.12) and Increase at (5, 7) % (87.57-105.59) then go down (at 9% =90.95), The roughness of the films shows increment by increasing doping at (0=0.458, 1%=14.6, 3%=22, 5%=24.3) but go down at 7 % =11.5, while the doped film by 9 % =26.8 SnO_2 have maximum values of roughness.

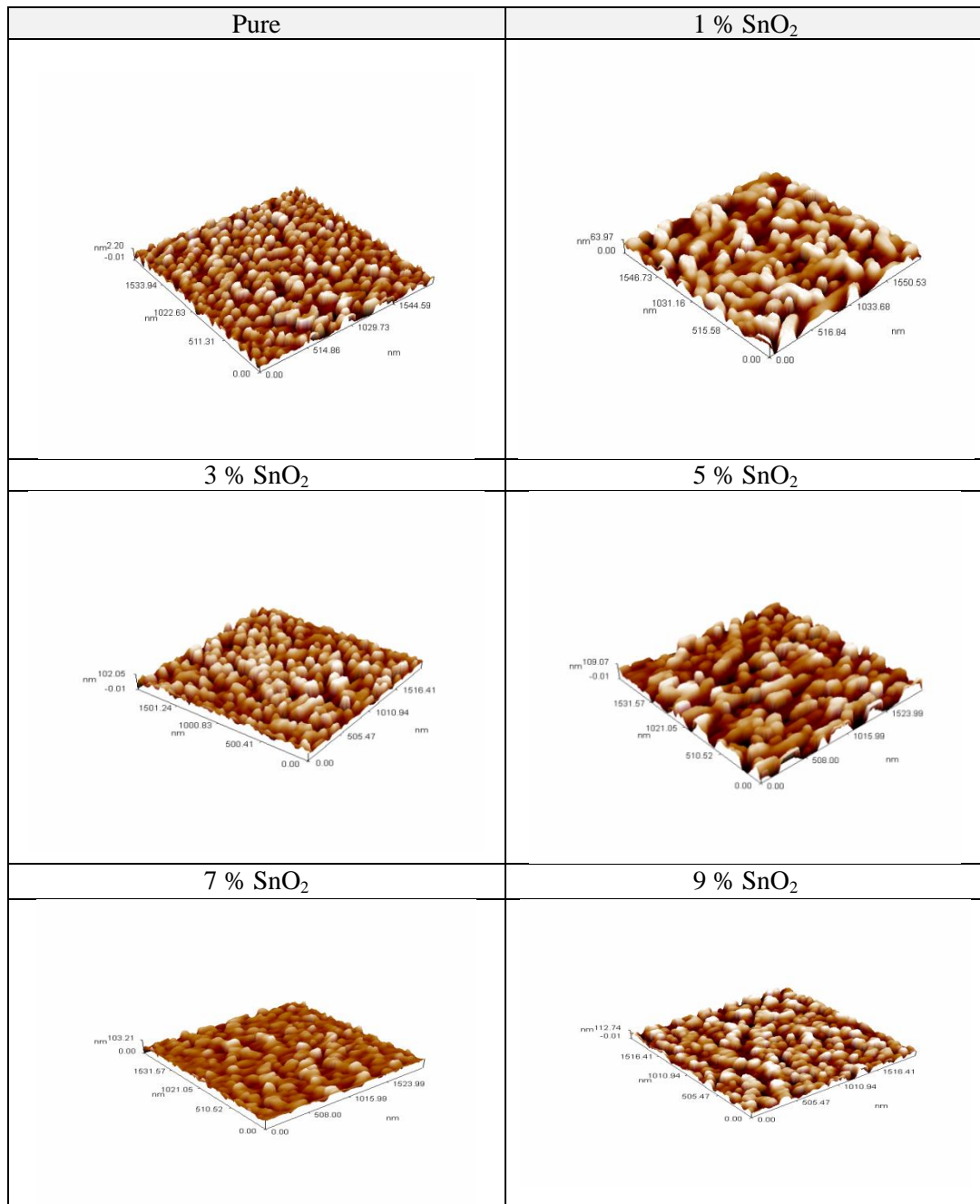


Fig.2: AFM images for of pure In_2O_3 thin film and In_2O_3 doped with SnO_2 at different doping ratio.

3- The Electrical properties

3-1 D.C conductivity

Fig. 3 shows the variation of $\ln(\sigma)$ with reciprocal temperature of In_2O_3 thin films prepared with different doping ratios of SnO_2 . From these figures it is evident that there are more than one conduction mechanism and hence more than one activation energy which reflects the polycrystalline structures of the prepared thin films. The activation energies were estimated according to Eqs. (3 and 4) and listed in Table 1. Indeed two activation energies can be observed for the pure and doped samples with 1 %, 3 %, 7 % while three activation energies for (5 and 9 %). On the other hand it is clear that the conductivity decreased as SnO_2 added to the host material but then get to rise. The continuous addition of SnO_2 lead to reduce the conductivity. The activation energy exhibit to change in reverse manner to that of conductivity. This results was expected since the activation energy is half of energy gap and can be attributed to same reasons i.e. the increment of the activation energy related to the creation of new states in the band gap which lead to visual reduction of energy gap while the reduction of activation energy is related to compensation effect of the added dopant. According to Davis and Mott model 1979 [15] the tails of localized states should be rather

narrow and extend a few length of tenths of an electron volt into the forbidden gap, and further more thus suggested of localized levels near the middle of the gap. This leads to different channels of conduction: E_{a1} is the activation energy required to transport electron from Fermi level to the extended states above the conduction band edge, E_{a2} is the activation energy required to transport electron from Fermi level to the localized below the conduction band edge. The increasing of doping ratio has significant effect on of the number on transport mechanisms of the $\text{In}_2\text{O}_3: \text{SnO}_2$ system. The variation of E_a of $\text{In}_2\text{O}_3: \text{SnO}_2$ thin films with doping ratio is illustrated in Table 1. It is clear from this table that the activation energies change in non regular manner with the increase of doping ratio. Indeed E_{a1} and E_{a2} increases as the dopant material added to the host system but then decreases with further addition of SnO_2 . The decreasing of activation energy with the increase of thickness is resulting from the effect of reduction of energy gap which in turn reduces the energy requires to transport the carriers from Fermi level to the conduction band. The appearance of third transport mechanism and third activation energy is related with reduction of degree of crystallinity which consequently reduces the grain size.

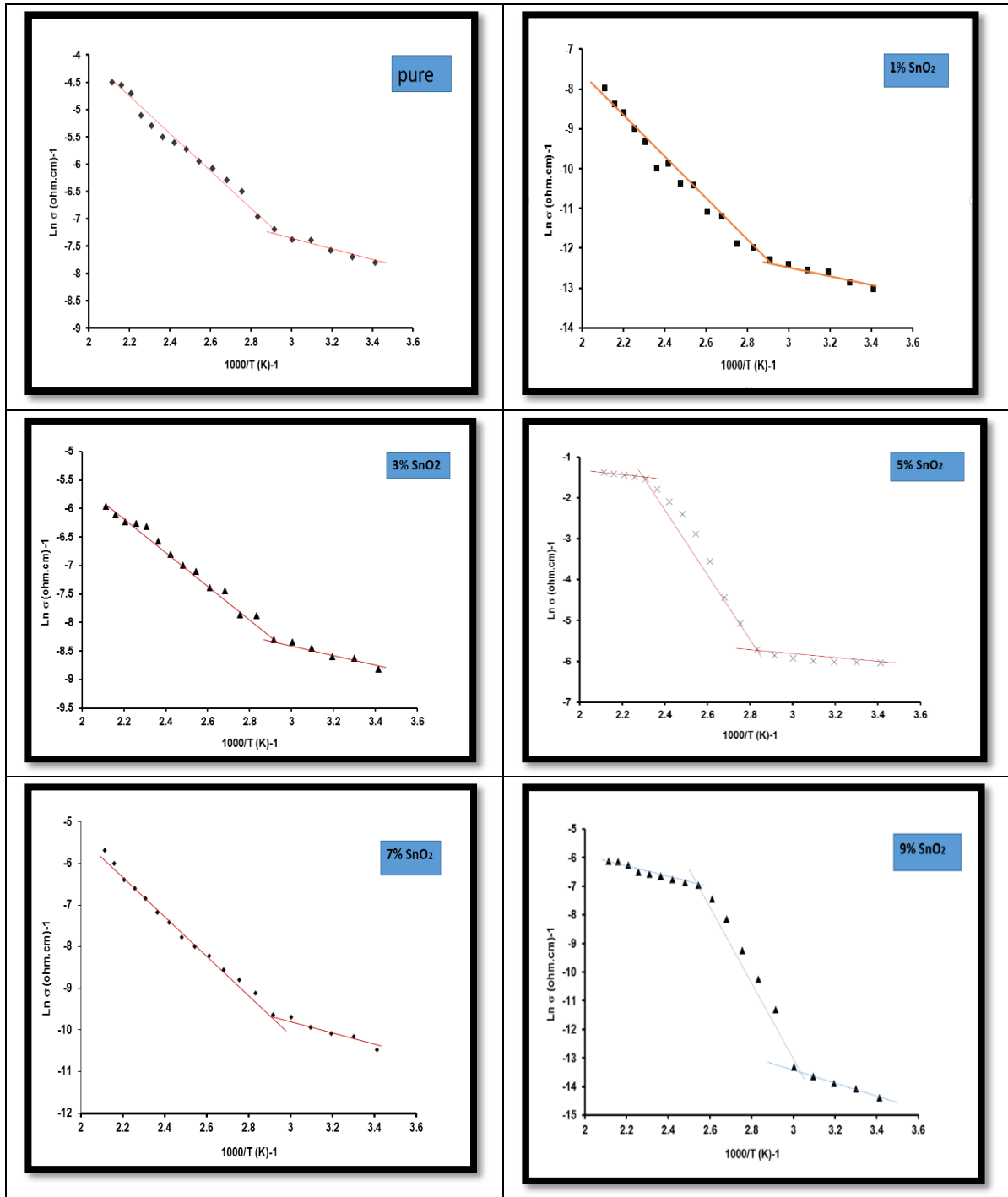


Fig.3: Plot of $\ln(\sigma)$ vs. $1000/T$ of pure In_2O_3 and doped with different ratio of SnO_2 deposited at R.T.

Table 1: D.C activation energies, their temperature ranges for pure In_2O_3 and doped with different ratio of SnO_2 deposited at R.T.

SnO ₂ (%)	Activation energies (eV)	Temp.Range (K)	σ (ohm.cm) ⁻¹
0	Ea ₁ 0.123	293-343	3.4x10 ⁻⁴
	Ea ₂ 0.282	343-473	
1	Ea ₁ 0.126	293-343	2.2x10 ⁻⁶
	Ea ₂ 0.465	343-473	
3	Ea ₁ 0.090	293-343	1.5x10 ⁻⁴
	Ea ₂ 0.377	343-473	
5	Ea ₁ 0.044	293-353	2.4x10 ⁻²
	Ea ₂ 0.417	353-443	
	Ea ₃ 0.068	443-473	
7	Ea ₁ 0.143	293-343	2.3x10 ⁻³
	Ea ₂ 0.403	343-473	
9	Ea ₁ 0.218	293-333	5.6x10 ⁻⁷
	Ea ₂ 1.175	333-393	
	Ea ₃ 0.178	393-473	

3- 2 Hall effect

Hall Effect measurements provided the valued of the carrier concentration (n_H), the type of charge carriers and Hall mobility (μ_H) for pure In_2O_3 and In_2O_3 doped with SnO_2 films at different doping ratio (1, 3, 5, 7 and 9) wt. % deposited on glass substrate were calculated. The negative sign of Hall coefficient indicates the

conductivity nature of the film are n-type. Hall measurements show that In_2O_3 thin film has a negative Hall coefficient (n type charge carriers) or n type semiconductor, [see Table 2]. The addition of SnO_2 to the host material has different effect on the type of the charge carries, i.e. most of the sample changed to p-type semiconductors while the residual remain n-type.

Table 2: Hall measurements of undoped and doped In_2O_3 thin films prepared with different SnO_2 dopant concentrations deposited at R.T.

SnO ₂ %	n (cm ⁻³)	μ_H (cm ² /V.s)	ρ (Ω .cm) *10 ⁴	σ (Ω .cm) ⁻¹	type	R_H (cm ³ /C)
0	-5.281E+10	1.769E+4	6.682E+3	1.497E-4	n	-1.182E+8
1	1.851E+12	1.655E+1	2.038E+5	4.906E-6	P	3.373E+6
3	1.101E+12	5.876E-5	7.374E+5	1.037E-11	P	5.668E+6
5	-1.465E+12	6.230E+2	16.828E+3	1.465E-4	n	-4.266E+6
7	9.196E+11	6.364E+1	1.067E+5	9.376E-6	P	6.788E+6
9	-1.569E+12	1.300E+2	1.441E+3	2.510E-5	n	-3.980E+6

4- The measurements sensing properties of pure and doped In_2O_3 with SnO_2 deposited on p-type Si for NO_2 oxidizing gas

Thin films of sample are examined for gas sensing using NO_2 at different

operation temperature beginning from (room temperature, 373, 473 and 573)K. Figs. 4-9 show the variation of resistance as a function of time with on/off gas valve.

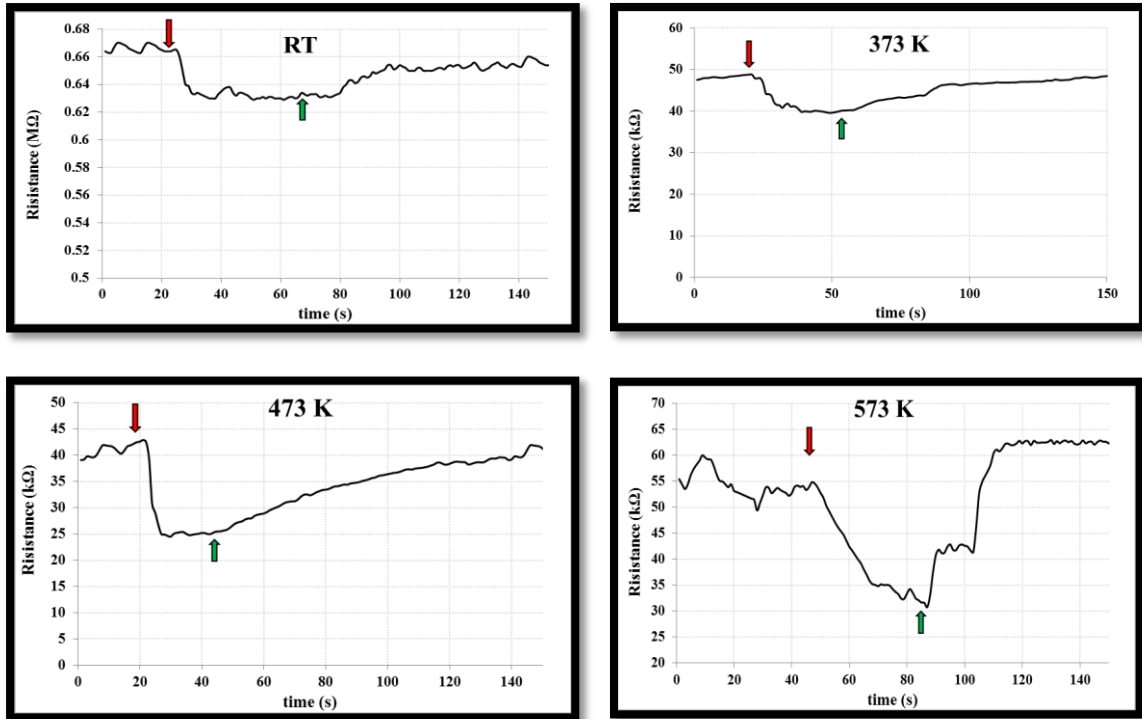


Fig. 4: Variation of resistance as a function of time for pure In_2O_3 films deposited on *p*-Si at different operating temperatures.

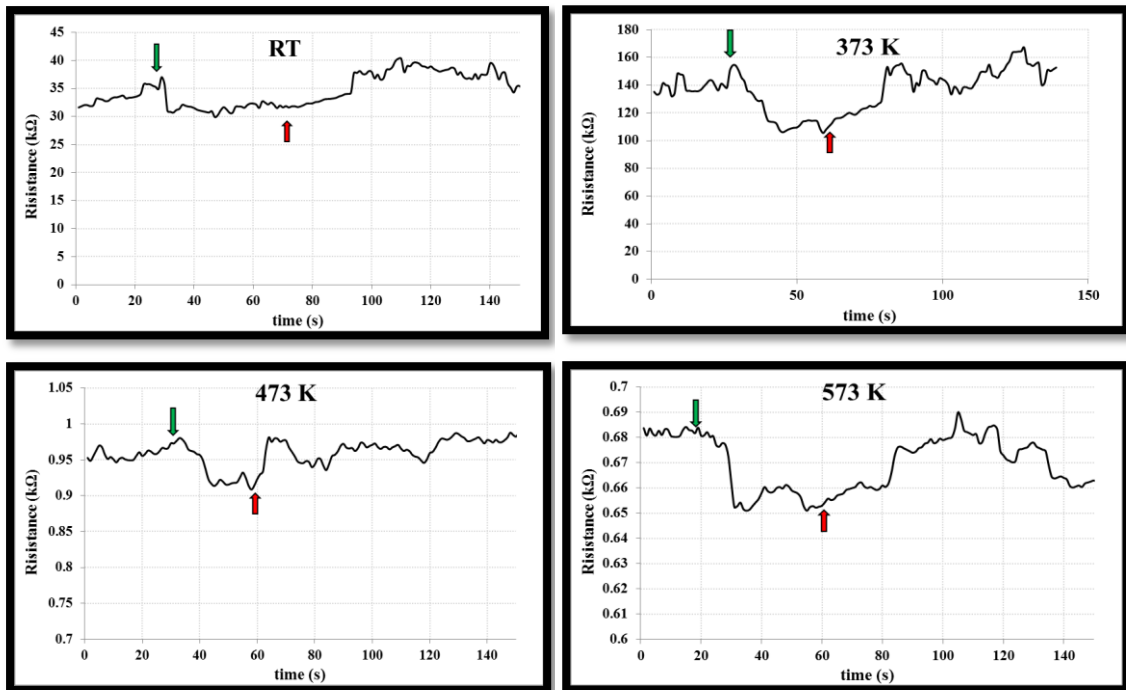


Fig. 5: Variation of resistance as a function of time for In_2O_3 films deposited on *p*-Si doped with 1 wt % SnO_2 ratio at different operating temperatures.

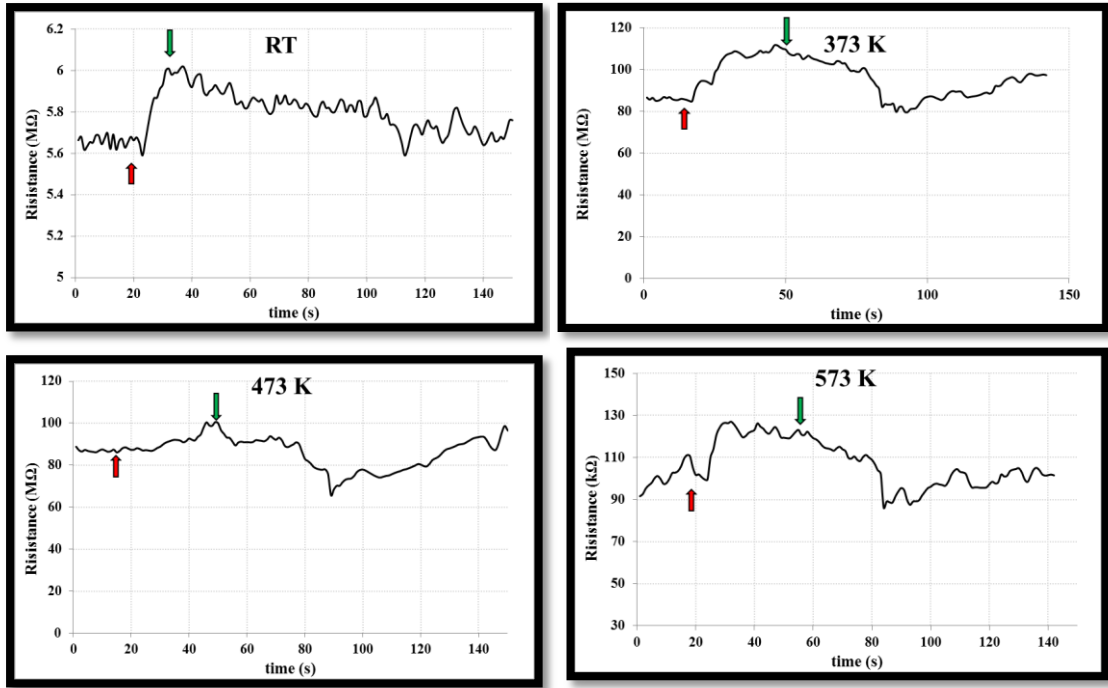


Fig. 6: Variation of resistance as a function of time for In_2O_3 films deposited on p- Si doped with 3 wt % SnO_2 ratio at different operating temperatures.

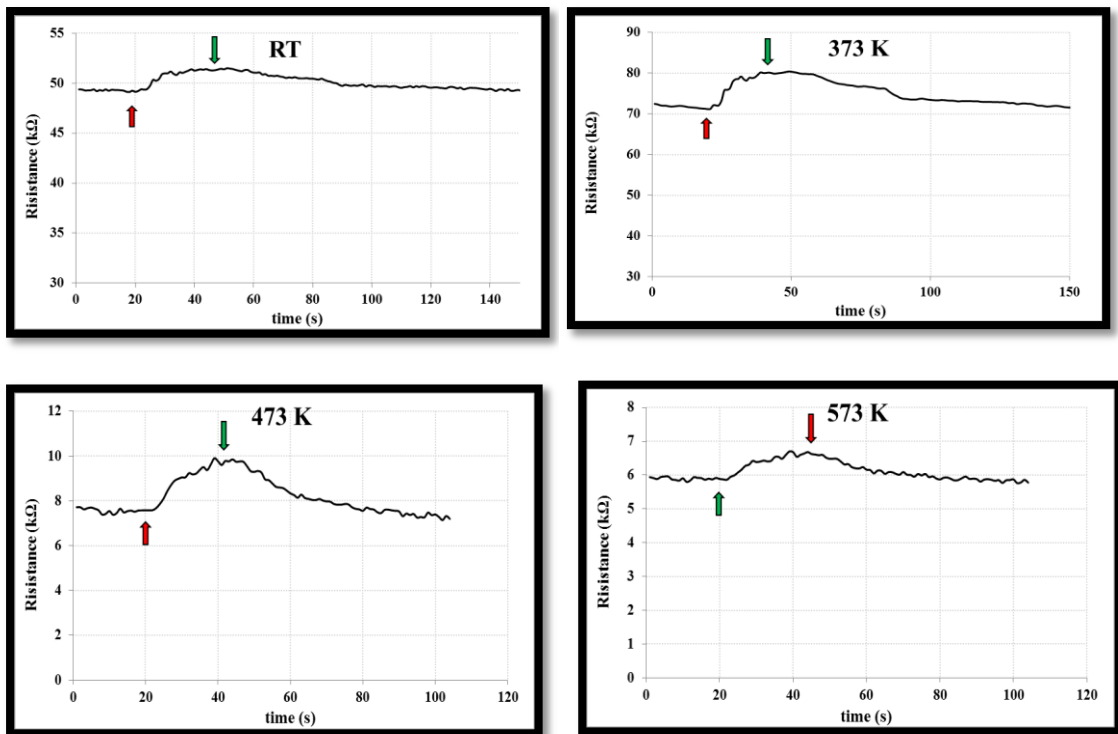


Fig. 7: The variation of resistance as a function of time for In_2O_3 films deposited on p- Si doped with 5 wt % SnO_2 ratio at different operating temperatures.

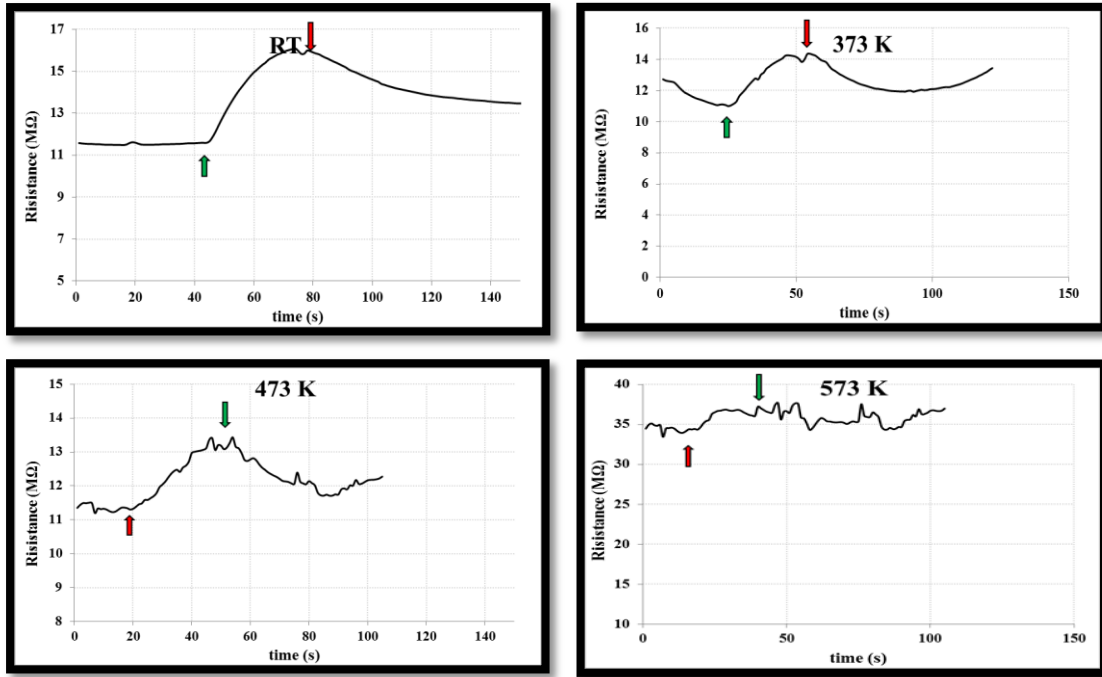


Fig.8: Variation of resistance as a function of time for In_2O_3 films deposited on p- Si with 7 wt %. SnO_2 ratio at different operating temperatures.

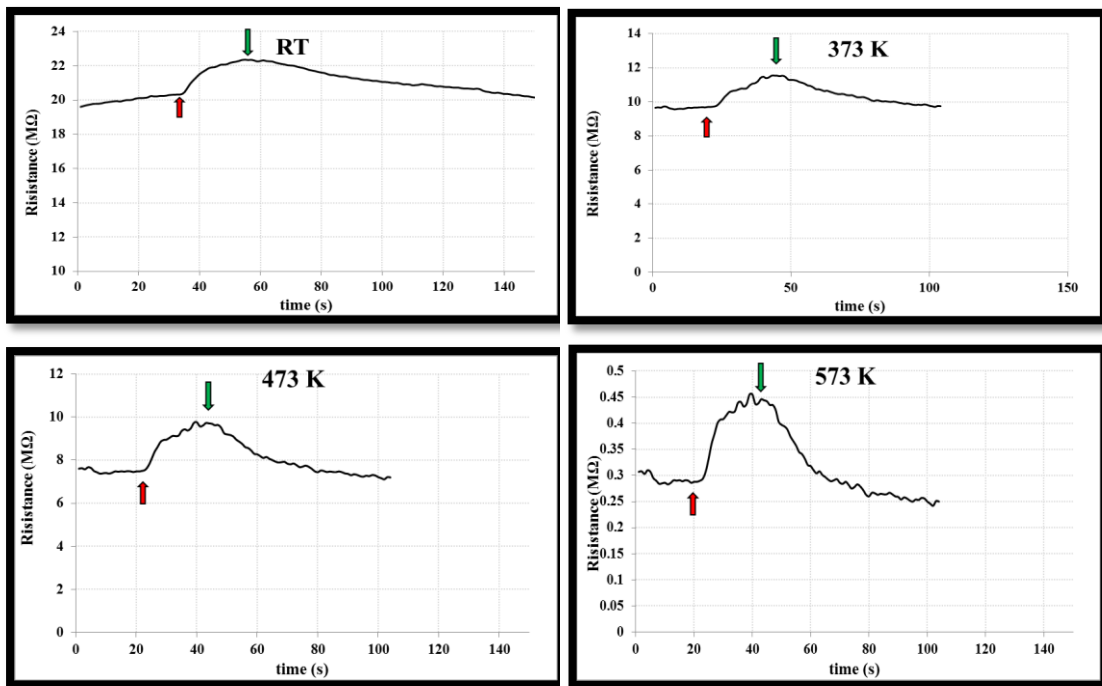


Fig. 9: Variation of resistance as a function of time for In_2O_3 films deposited on p- Si with 9 wt %. SnO_2 ratio at different operating temperatures.

It is clear from these figures that the resistance decrease with gas on for (pure and doped samples with 1% SnO_2). These figures show decreasing in the resistance value when their films

expose to NO_2 gas, (Gas on), then the resistance value back upward at the closure of the gas (Gas off). While the doped samples with (3, 5, 7 and

9) wt.% SnO₂ show an increase of the resistance with (gas on).

4-1 Effect of operation temperature on the sensor

Table 3 shows the operating temperature dependence of sensitivity for pure In₂O₃ and doped with different concentrations of SnO₂, which are deposited on p-type silicon substrates. It is clear that the sensitivity change in

non regular manner with both doping ratio and operating temperatures. In general the sensitivity increases with the increase of doping ration for temperatures 473 and 573 K while the sensitivity return to fall for low operating temperatures, i.e. R.T and 373 K. It is obvious the sensitivity values are lower that these values for gas sensors deposited on n-Si substrate.

Table 3: Operating temperature dependence of Sensitivity for un-doped and doped In₂O₃ doped with different concentrations of SnO₂ for NO₂ gas deposited on p-Si.

Operating Temp.(K)	SnO ₂					
	Doping Ratio					
	0 %	1 %	3 %	5 %	7 %	9 %
R.T	5.97	14.28	7.14	8.3	39.13	11
373	16.6	26.6	11.11	27	27.3	15
473	41.9	6.12	17.64	33.3	30.7	30.7
573	45.4	4.41	28	11.6	50	50

On the other hand it is clear that the sensitivity of the films increase with increasing of the operating temperature. Maximum point values for In₂O₃ films doped with the ratio (7 and 9) % SnO₂ are seen at temperature of (573K) which known as optimal temperature. At the optimal temperature, the activation energy may be enough to complete the chemical reaction. There is an increase and decrease in the sensitivity indicates the adsorption and desorption phenomenon of the gas.

4-2 Response and recovery times

Table 4 shows the relation between the response time and the recovery

time with different Tin oxide doping ratios at different operating temperatures of the undoped and doped In₂O₃ thin films. From the table can be observed increasing response time with increased of doping ration at room temperature, while it get to reduce at high operating temperatures (373, 473, and 573 K). Also the recovery time have the same manner, i.e it get to increase with doping ratio for low operating temperature i.e (R.T and 373 K) while it decreases with doping ratio for high operating temperatures (473 and 573 K).

Table 4: Response and recovery time of un-doped and doped In_2O_3 with different ratios of SnO_2 for NO_2 deposited on p-Si.

% SnO_2	Response time (s)				Recovery time (s)			
	Operating Temperature (K)				Operating Temperature (K)			
	R.T	373	473	573	R.T	373	473	573
0	10	25	10	30	25	40	70	30
1	12	15	10	8	22	23	10	30
3	10	20	25	20	60	30	25	30
5	20	22	20	20	32	45	25	20
7	25	10	25	18	30	60	25	33
9	15	20	25	18	50	60	25	33

The previous figure shows that the 1% SnO_2 doped samples exhibits a fast response speed (8 s) with recovery time (30 s) at 573 K this referred that a low doping ratio is the best to achieve fast response sensor. The quick response sensor for NO_2 gas may be due to faster oxidation of gas.

Conclusions

1- The prepared $In_2O_3:SnO_2$ alloys and thin films have polycrystalline structure with a cubic structure with a preferential orientation along (222) direction.

2-The average diameter and average roughness change in reverse manner with the increase of in tin oxide concentration. Maximum diameter and average roughness obtained are 105.59 and 26.8 nm respectively.

3-The results showed good correlation between structural, morphological and electrical properties was found. The increase of tin oxide to 3 and 5 % improves the crystallinity, increases the grain size and decreases the resistivity.

4-Maximum sensitivity obtained from $In_2O_3:SnO_2/p$ -Si thin films gas sensor (50) for tin oxide concentration 7% at 573 K.

5-Minimum response time obtains from $In_2O_3:SnO_2/p$ -Si thin films gas sensor were 8 sec at 573 K.

6-Increase of operating temperature enhanced the sensitivity of the prepared $In_2O_3:SnO_2$ thin films.

References

- [1] L. Filipovic and S. Selberherr, *Sensors*, 15 (2015) 7206-7227.
- [2] L. Trakhtenberg, G. Gerasimov, V.Gromov, T. Belysheva, O. Ilegbusi, *Sensors and Actuators B*, 169 (2012) 32-38.
- [3] M. Alam, D. Cameron, *Thin Solid Films*, 377-378 (2000) 455-459.
- [4] Y. Han, D. Kim, J. Cho, S. Koh, Y. Song, *Sol. Energy Mater. Sol. Cells* 65, (2001) 211-218.
- [5] G. Neri, A. Bonavita, G. Micali, G. Rizzo, E. Callone, G. Carturan, *Sens. Actuators B*, 132 (2008) 224-233.
- [6] J. Park, C. Buurma, S. Sivananthan, R. Kodama, W. Gao, T. Gessert, *Appl. Surf. Sci.*, 307 (2014) 388-392.
- [7] K.Tseng and Y. Lo, *Appl. Surf. Sci.*, 285 (2013) 157-166.
- [8] G. Mandayo, E. Castano, F. Gracia, A. Cirera, A. Cornet, J. Morante, *Sensors and Actuators B*, 95 (2003) 90-96.
- [9] J. McCue, J. Ying, *Chem. Mater.*, 19 (2007) 1009-1015.
- [10] J. B. Choi, J. H. Kim, K. A. Jeon, S. Y. Lee, *Mat. Science and Eng. B102* (2003) 376-379.
- [11] T.F. Stoica, V.S. Teodorescu, M.G. Blanchin, M. Gortner,

M.Losurdo, M. Zaharescu, Mater. Sci. Eng., B101 (2003) 222.

[12] L. Kerkache, A. Layadi, A. Mosser, Journal of Alloys and Compounds, 485 (2009) 46-50.

[13] M. Nisha, M. K. Jayaraj, Appl. Surf. Sci., 255 (2008) 1790-1795.

[14] H.L. Ma, D.H. Zhang, P. Ma, S.Z. Win, S.Y. Li, Thin Solid Films, 263 (1995) 105-110.

[15] N. Mott. and E. Davis'Electronic Process in Non-crystalline Materials', 2nd ed., University Press, Oxford (1979), P.858.